GMPS #831698, VOL 20, ISS 4

A PAIR-APPROXIMATION MODEL FOR SPATIAL PATTERNS IN TREE POPULATIONS WITH ASYMMETRICAL RESOURCE COMPETITION

Josep L. Garcia-Domingo and Joan Saldaña

QUERY SHEET

This page lists questions we have about your paper. The numbers displayed at left can be found in the text of the paper for reference. In addition, please review your paper as a whole for correctness.

Q1: Au: Please confirm author names, order, and affiliations
Q2: Au: Please provide a title for the Appendix

TABLE OF CONTENTS LISTING

The table of contents for the journal will list your paper exactly as it appears below:

A Pair-Approximation Model for Spatial Patterns in Tree Populations with Asymmetrical Resource Competition
Josep L. Garcia-Domingo and Joan Saldaña

3b2 Version Number : 7.51c/W (Jun 11 2001)
File path : P:/Santype/Journals/TandF_Production/GMPS/v20n4/GMPS831698/GMPS831698.3d
Date and Time : 29/08/13 and 17:08

Mathematical Population Studies, 20:1–17, 2013

ISSN: 0889-8480 print/1547-724X online
DOI: 10.1080/08898480.2013.831698

Routledge
Taylor & Francis Group

A PAIR-APPROXIMATION MODEL FOR SPATIAL PATTERNS IN TREE POPULATIONS WITH ASYMMETRICAL RESOURCE COMPETITION

Q1

Josep L. Garcia-Domingo
Departament d'Economia i Empresa, Universitat de Vic, Spain

Joan Saldaña
Departament Informàtica i Matemàtica Aplicada, Universitat de Girona, Spain

A pair-approximation model for the spatial dynamics of a height-structured tree population is defined on a regular lattice where each site can be in one of three states: empty (gap site), occupied by an immature tree, and occupied by a mature tree. The nonlinearities are associated with resource competition effects of mature trees on immature ones (asymmetric competition) affecting the mortality of the latter but not their growth. The survival-extinction transition of the forest is expressed; the early dynamics of colonization are described in terms of local densities. Predictions of the pair approximation model are compared with results from numerical simulations of cellular automata.

Keywords: cellular automata; early dynamics; lattice models; pair approximation; resource competition; spatial forest dynamics

1. INTRODUCTION

As in the study of other problems in biology and chemistry, in the 1970s partial differential equations (PDE) were introduced to model the reaction and diffusion processes characterizing vegetation and forest dynamics. This classical framework offers a large-scale description of systems where population densities vary in a continuous space. However, reaction-diffusion PDE models neglect small-scale spatial correlations and, when differences among individuals are significant and local interactions matter, other frameworks are more appropriate (Cronhjort, 2000; Chen et al., 2002). Such are spatially explicit individual-based models, cellular automata, and moment-based models (Gratzer et al., 2004). When individual differences matter but the population spatial distribution, as in forest exploitations, does not, continuously size-structured population dynamics are described by hyperbolic PDEs (Metz and Diekmann, 1986). Goetz et al. (2011) considered this situation in the study of optimal control problems of forest management, an optimization issue which is usually formulated in terms of discrete age-class models (Tahvonen, 2004).

Address correspondence to Joan Saldaña, Departament Informàtica i Matemàtica Aplicada, Universitat de Girona, Girona E-17071, Spain. E-mail: jsaldana@ima.udg.edu

Stochastic lattice models (Silvertown et al., 1992; Harada and Iwasa, 1994; Childress, 1997) have been used since the 1990s for studying spatial vegetation dynamics (Tilman and Kareiva, 1997; Bascompte and Solé, 1997; Hanski, 1999). Aspects of these dynamics that have been considered so far are, for instance, the size distribution of gaps (Solé and Manrubia, 1995; Kubo et al., 1996; Schlicht and Iwasa, 2004; Pagnutti et al., 2007), species richness (Hubbell et al., 1999), different neighborhoods for reproduction and competition (Ellner, 2001), regeneration waves (Schlicht and Iwasa, 2007), and spatially correlated disturbances (Hiebeler, 2005).

Garcia-Domingo and Saldaña (2011) extended the pioneering works of Iwasa and co-authors on gap-occupancy models for forest spatial dynamics in order to include a simple vertical layering. This vertical structure of the forest consists of three layers: the canopy (the tallest layer, composed of mature trees), the understory (the layer composed of saplings of canopy trees), and the shrub layer (the lowest layer of woody vegetation). This vertical stratification was also considered in Adams et al. (2007) in the context of interspecific height-structured competition for light. Although simple, it allows for a new type of local interaction among individuals, namely the asymmetrical competition for nutrients and sunlight. Manrubia and Solé (1997) and Pagnutti et al. (2005) dealt with lattice models of forest dynamics with a richer vertical layering; Solé et al. (2005) addressed the interaction between dispersal strategies and vertical forest stratification. These authors used simulations of cellular automata. In contrast, Garcia-Domingo and Saldaña (2011) theorize on a stochastic lattice forest with a vertical layering, using the so-called pair approximation (Harada et al., 1994, 1995; Rand, 1999; Keeling, 1999; Sato and Iwasa, 2000), which consists in deriving the differential equations describing the dynamics of the total number of ordered pairs ij of adjacent sites which are in state i and j.

The novelty of the model we present is the assumption of the existence of asymmetrical competition between mature and immature trees affecting the mortality of the latter. This sort of competition is based on the fact that mature trees have a larger root system than immature ones, are higher, and have larger crowns. In ecology, it is the so-called self-thinning process, whereby during a stand development, the density of trees decreases as the stand biomass increases. This process is most easily observed in even-aged stands. Li et al. (2000) claimed that it emerges from the ecological interactions among individuals (or local spatial field effects). In this sense, competition for light is one of the most important interactions in plant and tree populations, and the existence of an interspecific trade-off between high survivorship under low light availability (shade-tolerant species) against rapid growth under high light availability (shade-intolerant or light-demanding species) is established by Martin et al. (2010). However, in some tree species, mortality remains constant across different values of the (radial) growth rate in dense self-thinning stands, indicating that mortality can be driven by factors different from light competition in these species (Dekker et al., 2009). Martin et al. (2010) show the existence of exotic invading tree species combining very high growth rates with moderately high shade tolerance, diverging from the growth-survival trade-off pattern of the native species. We shall consider that competition primarily affects the survivorship of saplings but not their growth rate, which is assumed to remain constant for different levels of light. This can be the case of shade-tolerant species for which the effects of competition for light are small compared with those competing for resources (e.g., space, nutrients, water).

In terms of the model, the asymmetrical competition is modeled by an additional mortality of immature trees, which is assumed to be proportional to the total number of neighboring mature trees.

2. MODEL

The forest region is represented by a two-dimensional regular lattice of N stands or sites. Each site can be empty (O, a gap site), occupied by a mature tree (M) or an immature tree (I). Transitions among these states correspond to three vital processes: birth, growth, and death (Figure 1). Mature trees produce seeds which germinate in nearby empty sites giving rise to immature trees (saplings). The latter can die, leaving an empty site, or grow and become a mature tree. Similarly, mature trees can die, creating new gaps.

Due to the local interactions among trees, the rates of these processes are not constant but rather depend on the states of the neighboring sites. For instance, the recruitment of immature trees depends on the total number of mature trees around empty sites because the more numerous mature trees surrounding a gap, the higher the probability of seeds germinating in this gap. In turn, the mortality of immature trees is increased by the presence of neighboring mature trees because of asymmetrical competition effects. In addition to natural mortality, mature trees can die due to wind disturbances which cause their fall. This additional mortality is proportional to the total number of gap sites surrounding a mature tree. Immature trees cannot produce seeds and are insensitive to wind stress thanks to a higher flexibility.

We denote by $[O]$, $[I]$, and $[M]$ the total number of gaps, immature trees, and mature trees, respectively, in a two-dimensional regular lattice of N sites. The total number of nearest neighbors per site in the lattice is denoted by z. For a fixed site x, $Q_x(i)$ denotes the total number of the nearest neighbors of x which are in state i at time t ($0 \le Q_x(i) \le z$). The transitions between states for every site x are symbolized by:

$$\begin{aligned} &1.\text{recruitment} : O \xrightarrow{R_x} I, \\ &2.\text{growth} : I \xrightarrow{g} M, \\ &3.\text{death} : \begin{cases} I \xrightarrow{D_x^I} O, \\ M \xrightarrow{D_x^M} O, \end{cases} \end{aligned}$$

where R_x, G_x, D_x^I, and D_x^M are the corresponding transition rates. The growth rate g of immature trees is assumed to be constant whereas the rest of rates are defined as:

$$R_x = \frac{\beta}{z} Q_x(M), \quad D_x^I = d_I + \frac{\mu}{z} Q_x(M), \quad D_x^M = d_M + \frac{\delta}{z} Q_x(O), \tag{1}$$

where the recruitment is proportional to the total number of neighboring mature trees of a gap site, β/z is the per neighbor-pair fertility rate of a mature tree, d_I is the natural mortality rate of immature trees, μ/z is the competition effect caused by a neighboring mature tree on an immature tree. The natural mortality rate of mature trees is d_M, and

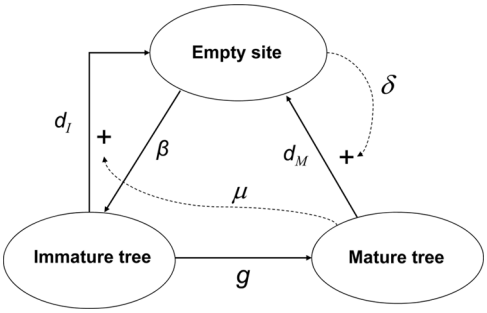

Figure 1. Scheme of the transitions among states and the interactions between neighboring sites assumed in the forest model. Doted arrows pointing to a plus sign (+) represent an additional contribution to the transition rate caused by the presence of neighboring sites in state M around immature trees, and in state O around mature trees.

δ/z is the induced mortality due to the presence of a gap in the neighborhood of a mature tree. Therefore, when all neighboring sites are gaps, the induced mortality is equal to δ, the so-called wind disturbance in Kubo et al. (1996).

We use the pair approximation technique to analyze the dynamics of structured populations, which are spatially distributed in regular lattices (Rand, 1999; Keeling, 1999; Sato and Iwasa, 2000). The idea of this method is to extend the mean-field equations for the total number of sites in different states (O, M, and I) by incorporating pairwise interactions between neighboring sites which define the pairs. To approximate the total number of triples arising in the equation for pairs, we assume that the presence of a site in a given state at one end of a triple does not affect the probability of the state of the site at the other end of the triple. The system of equations for the total number of different types of pairs is closed under this triple closure.

Let $[ij]$ be the total number of ordered pairs of adjacent sites in states i and j. Because only nearness in space defines pairs, $[ij]=[ji]$ and pairs of adjacent sites in the same state i are counted twice in $[ii]$. Let $[ijk]$ be the total number of ordered triples whose sites are in states i, j, and k. Averaging over the lattice, the mean value of the transition rates R_x, D_x^I, and D_x^M are given by:

$$R=\frac{\beta}{z}\frac{[OM]}{[O]},\quad D_I=d_I+\frac{\mu}{z}\frac{[IM]}{[I]},\quad \text{and}\quad D_M=d_M+\frac{\delta}{z}\frac{[OM]}{[M]}. \tag{2}$$

Using these averages, the differential equation for the total number of immature trees is:

$$[I]\prime(t)=\frac{\beta}{z}\frac{[OM](t)}{[O](t)}[O](t)-\left(g+d_I+\frac{\mu}{z}\frac{[IM](t)}{[I](t)}\right)[I](t). \tag{3}$$

Similarly, one can compute the average total number of neighbors in a given state for the sites belonging to a given type of pair. For example, the mean total number of neighboring mature trees of the gap in (I, O)-pairs is given by $[IOM]/[IO]$.

. Proceeding along the same lines for the other site and pair variables, the system of differential equations governing the dynamics of sites and pairs is:

$$[I]'(t) = -(g + d_I)\,[I](t) + \frac{\beta}{z}\,[OM](t) - \frac{\mu}{z}[IM](t) \tag{4}$$

$$[M]'(t) = g\,[I](t) - d_M\,[M](t) - \frac{\delta}{z}\,[OM](t) \tag{5}$$

$$[II]'(t) = 2\,\frac{\beta}{z}\,[IOM](t) - 2(g + d_I)\,[II](t) - 2\frac{\mu}{z}[IIM](t) \tag{6}$$

$$\begin{aligned}[IM]'(t) = {} & \frac{\beta}{z}\,[OM](t) + g\,[II](t) - (d_I + d_M + g)\,[IM](t) - \frac{\mu}{z}\,[IM](t) \\ & + \frac{\beta}{z}\,[MOM](t) - \frac{\delta}{z}\,[IMO](t) - \frac{\mu}{z}\,[MIM](t)\end{aligned} \tag{7}$$

$$[MM]'(t) = 2\,g\,[IM](t) - 2\,d_M\,[MM](t) - 2\,\frac{\delta}{z}\,[OMM](t). \tag{8}$$

This system of equations is closed by introducing a pair approximation (PA) for the total number of triples. Here we use the usual PA (Kubo et al., 1996), which is given by:

$$[ijl] = k\,\frac{[ij][jl]}{[j]}, \tag{9}$$

with $k = \frac{z-1}{z}$, although other values of k are possible (Rand, 1999). Under this approximation, the expected total number of (i, j, l)-triples in the lattice is equal to the total number of neighbors of those j-sites in (i, j)-pairs, $(z-1)[ij]$, times the conditional probability that a j-site has a neighbor in state l, $[jl]/(z[j])$. This PA and the fact that, for $x = O, I, M$, $z[x] = [xI] + [xM] + [xO]$ amount to the approximations for the total number of triples of each type:

$$[IIM] = k\,\frac{[II][IM]}{[I]}, \tag{10}$$

$$[IOM] = k\,\frac{[IO][OM]}{[O]} = k\,\frac{(z[I] - [IM] - [II])(z[M] - [IM] - [MM])}{N - [I] - [M]}, \tag{11}$$

$$[MIM] = k\,\frac{[IM]^2}{[I]}, \tag{12}$$

$$[MOM] = k\,\frac{[OM]^2}{[O]} = k\,\frac{(z[M] - [IM] - [MM])^2}{N - [I] - [M]}, \tag{13}$$

$$[IMO] = k\,\frac{[IM][MO]}{[M]} = k\,\frac{[IM](z[M] - [IM] - [MM])}{[M]}, \tag{14}$$

$$[OMM] = k\frac{[OM][MM]}{[M]} = k\frac{(z[M] - [IM] - [MM])[MM]}{[M]}. \tag{15}$$

The nonlinearities introduced by the PA lead to the existence of singularities when the system is linearized around the trivial equilibrium $[I]^* = [M]^* = [II]^* = [IM]^* = [MM]^* = 0$. To remove these singularities, we re-scale the state variables using the fact that the total number of immature trees approaches 0 at the same rate as that of mature trees (see section 3.2).

3. EXTINCTION EQUILIBRIUM

One of the basic aspects of the dynamics of a population model is the stability of the trivial equilibrium. From an ecological point of view, this equilibrium is reached either when a population of trees experiences a change of (exogenous) environmental conditions and goes extinct, or when an initial colonization of an empty area fails to progress. In the first case, we think of a change in the value of one or more parameters and are interested in the extinction-survival transition curve. In the second case, we are interested in the early dynamics with initial conditions close to the trivial equilibrium. In either case, we refer to the trivial equilibrium as "the extinction equilibrium."

3.1. Existence of an Extinction Threshold

The main tuning parameter in the extinction-survival transition curve (or surface) is the wind disturbance δ with δ_c denoting its critical value, corresponding to the extinction threshold of the system. Adding Eq. (4) and (5) we obtain

$$\frac{d}{dt}([I](t) + [M](t)) = -\left(d_I[I](t) + d_M[M](t) + \frac{\mu}{z}[IM](t)\right) + \frac{\beta - \delta}{z}[OM](t) \tag{16}$$

$$< -d_m([I](t) + [M](t)) + \frac{\beta - \delta}{z}[OM](t), \tag{17}$$

where $d_m := \min\{d_I, d_M\} > 0$. Hence, the total number of trees $[I] + [M]$ tends exponentially to 0 as $t \to \infty$ for $\delta \geq \beta$, regardless of the values of the other mortality rates d_I, d_M, and μ. The tree population survival is then only possible for $\delta < \delta_c < \beta$. Moreover, when δ is large enough, the competition-induced mortality μ is also used as a tuning parameter. In this case, there exists a critical value μ_c such that for $\mu > \mu_c$ the tree population goes to extinction.

Assuming the existence of a unique nonextinction equilibrium for each $\delta < \delta_c$, we follow the branch of these equilibria toward the bifurcation point by taking $\delta \to \delta_c^-$. The value of the extinction threshold δ_c depends on other parameters. This dependence defines the survival-extinction transition surface in the parameter space: $\delta_c = \delta_c(\beta, g, d_I, d_M, \mu)$. To obtain this transition surface numerically, we proceed using the following steps (Garcia-Domingo and Saldaña, 2011):

1. At a nontrivial equilibrium, isolate $[IM]^*$ and $[MM]^*$ in terms of $[I]^*$ and $[M]^*$ from Eq. (4) and (5). For $\mu > 0$,

$$\begin{pmatrix} [IM]^* \\ [MM]^* \end{pmatrix} = \frac{z}{\mu\delta} \begin{pmatrix} \beta g - \delta(g + d_I) & -\beta d_M \\ \delta d_I - (\beta - \delta + \mu)g & \beta d_M + \mu(\delta + d_M) \end{pmatrix} \begin{pmatrix} [I]^* \\ [M]^* \end{pmatrix}, \quad (18)$$

and substitute their expressions into the other model equations. The condition $\beta g > \delta(g + d_I)$ is necessary for $[IM]^* > 0$ and implies $\beta > \delta$.

2. Impose that $[IM]^* > 0$ and $[MM]^* > 0$ at any nontrivial equilibrium to obtain, from System (18), the lower and upper bounds of $[I]^*/[M]^*$:

$$0 < \frac{\beta d_M}{\beta g - \delta(d_I + g)} < \frac{[I]^*}{[M]^*} < \frac{\beta d_M + \mu(d_M + \delta)}{(\beta + \mu)g - \delta(g + d_I)}. \quad (19)$$

3. Check that the inequality between the previous bounds amounts to

$$R_0^{MF} := \frac{g}{(g + d_I)} \frac{\beta}{(d_M + \delta)} > 1, \quad (20)$$

which is a necessary (but not sufficient) condition on the values of the parameters for the existence of a nontrivial equilibrium. Here R_0^{MF} corresponds to the basic reproduction number obtained by decoupling Eq. (4) and (5) from Eq. (6), (7), and (8) using the mean-field approximation for the total number of pairs, that is, introducing the approximation $[ij] \approx z[i][j]/N$ for the total number of pairs $[ij]$. R_0^{MF} is an upper bound of the true value of R_0 and overestimates the population growth rate (Garcia-Domingo and Saldaña, 2011).

4. Isolate $[II]^*$ in terms of $[I]^*$ and $[M]^*$ from Eq. (6) and check that $\lim_{\delta \to \delta_c^-} [II]^*/(z[I]^*) = 0$ using that $[I]^* + [M]^* \to 0^+$ as $\delta \to \delta_c^-$.
5. Divide Eq. (7) and (8) at equilibrium by $z[M]^*$ and take the limit as $\delta \to \delta_c^-$ to obtain a system of equations valid at the bifurcation point:

$$f_1(C, \delta_c, \mu, \beta, d_I, d_M, g) = 0 \quad (21)$$

$$f_2(C, \delta_c, \mu, \beta, d_I, d_M, g) = 0, \quad (22)$$

where $C = \lim_{\delta \to \delta_c -} ([I]^*/[M]^*)$ is a positive constant thanks to Eq. (19).

6. Give values to the parameters satisfying the condition $R_0^{MF} > 1$ and find the critical values δ_c and C numerically. This condition and Eq. (21) and (22) determine the survival-extinction transition surface.

In the numerical solution of System {(21),(22)}, δ_c depends on other parameters of the model. In particular, as we already proved at the beginning of this section, the top right panel of Figure 2 shows that $\delta_c < \beta$ using β as a parameter. Alternatively, we solve System {(21),(22)} for $\mu = \mu_c$ with $C = \lim_{\mu \to \mu_c}([I]^*/[M]^*) > 0$ and obtain the survival-extinction transition surface $\mu_c = \mu_c(\beta, g, d_I, d_M, \delta)$ as shown in Figure 3 for a particular choice of the parameters values.

3.2. Stability of the Extinction Equilibrium

To study the linear stability of the extinction equilibrium we transform System {(4),(5),(6), (7),(8)} to get rid of the singularities around this equilibrium.

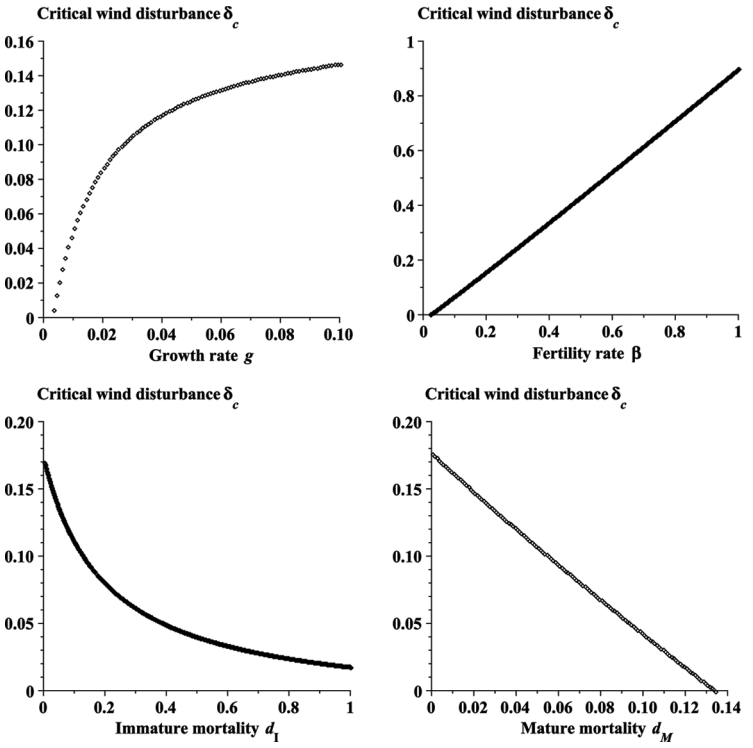

Figure 2. Survival-extinction transition curves. Critical wind disturbance δ_c against changes in the growth rate g (top left panel), in the fertility rate β (top right panel), in the immature mortality d_I (bottom left panel), and in mature mortality d_M (bottom right panel). Parameters: $\mu = 0.1$, $d_I = d_M = 0.01$ (except when one of them is the tuning parameter), $\beta = 0.2$ (except in the top right panel), $g = 0.2$ (except in the top left panel).

As in Garcia-Domingo and Saldaña (2011), this is done by re-scaling the original variables:

$$x = \frac{[I]}{[M]}, \quad y = [M], \quad u = \frac{[II]}{z[M]}, \quad v = \frac{[IM]}{z[M]}, \quad w = \frac{[MM]}{z[M]}. \tag{23}$$

Writing u as $[II]/(z[I])\cdot x$, any admissible solution must satisfy $u < x$. According to these re-scaled variables and as $[OM]/(z[M]) = 1 - v - w$, the system of differential 240
equations is:

$$\begin{aligned} x'(t) = {} & \beta(1 - v(t) - w(t)) - \mu v(t) - (g(1 + x(t)) + d_I - d_M \\ & - \delta(1 - v(t) - w(t)))x(t) \end{aligned} \tag{24}$$

$$y'(t) = (gx(t) - d_M - \delta(1 - v(t) - w(t)))y(t) \tag{25}$$

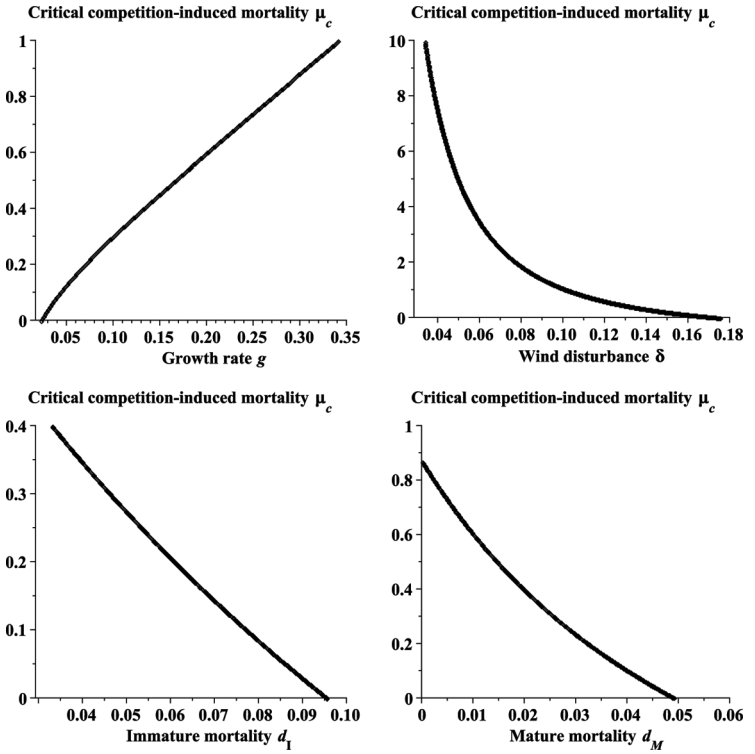

Figure 3. Survival-extinction transition curves. Critical competition-induced mortality μ_c against changes in the growth rate g (top left panel), in the fertility rate β (top right panel), in the immature mortality d_I (bottom left panel), and in mature mortality d_M (bottom right panel). Parameters: $\beta = 0.2$, $d_I = d_M = 0.01$ (except when one of them is the tuning parameter), $g = 0.2$ (except in the top left panel), and $\delta = 0.12$ (except in the top right panel).

$$u'(t) = 2k\beta \frac{(1 - v(t) - w(t))(x(t) - u(t) - v(t))}{N - y(t)(x(t) + 1)} y(t) - (g(2 + x(t)) + 2d_I + 2k\mu \frac{v(t)}{x(t)} - d_M - \delta(1 - v(t) - w(t))) u(t) \tag{26}$$

$$v'(t) = \frac{\beta}{z}(1 - v(t) - w(t)) + g\,u(t) - (g(1 + x(t)) + d_I + \frac{\mu}{z} - \frac{\delta}{z}(1 - v(t) - w(t))) v(t) + k\beta \frac{(1 - v(t) - w(t))^2}{N - y(t)(x(t) + 1)} y(t) - k\mu \frac{v^2(t)}{x(t)} \tag{27}$$

$$w'(t) = 2g v(t) - (g x(t) + d_M + (z - 2)\frac{\delta}{z}(1 - v(t) - w(t))) w(t). \tag{28}$$

The first component x^* of an equilibrium of System {(24),(25),(26),(27),(28)} corresponding to an extinction equilibrium of the original system ($y^* = [M]^* = 0$) is always strictly positive. If x approaches 0, $v'(t)$ becomes negative and unbounded; 250

the positivity of $x'(t)$ follows because $v(t)$ also tends to 0, and the first term in the right hand side of Eq. (24) becomes the dominant one. This guarantees that $x(t) > 0$ for all $t > 0$, which implies that $x^* > 0$ at any extinction equilibrium, and that Eq. (27) for $v'(t)$ has no singularities close to this equilibrium.

Whenever $y^* = 0$, any equilibrium of System {(24),(25),(26),(27),(28)} is of the form $(x^*, 0, 0, v^*, w^*)$ with $x^*, v^*, w^* > 0$. From Eq. (24) at equilibrium, $g(1 + x^*) + d_I - d_M - \delta(1 - v^* - w^*) = \beta(1 - v^* - w^*)/x^* - \mu v^*/x^*$. Upon substitution into the right-hand side of Eq. (26), $(g + d_I + \beta(1 - v^* - w^*)/x^* + (z - 2)/z \cdot \mu v^*/x^*)u^* = 0$ which implies $u^* = 0$ because $z \geq 2$ and $v^* + w^* < 1$ by the definition of the re-scaled variables. Substituting $y^* = u^* = 0$ into Eq. (27), $v^* > 0$ because of the strict positivity of the first term in the right-hand side of this equation, which implies $v'(t) > 0$ for $v \approx 0$. At the survival-extinction transition, the equilibrium is given by $(x^*, y^*, u^*, v^*, w^*) = (C, 0, 0, \alpha_2^c, \alpha_3^c)$ with C given by the solution of Eq. (21) and (22), $\alpha_2^c := \lim_{\delta \to \delta_c} [IM]^*/(z[M]^*)$ and $\alpha_3^c := \lim_{\delta \to \delta_c} [MM]^*/(z[M]^*)$.

Local stability of the extinction equilibrium is examined by linearizing System {(24), (25),(26),(27),(28)} around the equilibrium $(x^*, 0, 0, v^*, w^*)$ and computing the eigenvalue of the corresponding Jacobian matrix J^* with the largest real part, here denoted by λ_1. This eigenvalue turns out to be real and coincides with the stability modulus of J^*. In particular, both factors on the right-hand side of Eq. (25) must be equal to 0 at the bifurcation equilibrium so that $J^*(C, 0, 0, \alpha_2^c, \alpha_3^c)$ has a row whose elements are all 0 and, subsequently an eigenvalue equals 0. Figure 4 shows λ_1 parameterized by δ and μ. From Figure 4, as expected, $\lambda_1 \to 0$ as $\delta \to \delta_c$ (left panel) or $\mu \to \mu_c$ (right panel). As λ_1 crosses 0, the computation of the equilibria of System {(24),(25),(26),(27),(28)} shows that this system undergoes a transcritical bifurcation at the equilibrium $(x^*, y^*, u^*, v^*, w^*) = (C, 0, 0, \alpha_2^c, \alpha_3^c)$ with an exchange of stability between the only admissible ($u^* < x^*$) non-extinction ($y^* > 0$) equilibrium existing for $\delta < \delta_c$ and the extinction one. For $\delta > \delta_c$, the second component of the non-trivial equilibrium becomes negative and this equilibrium has no biological meaning.

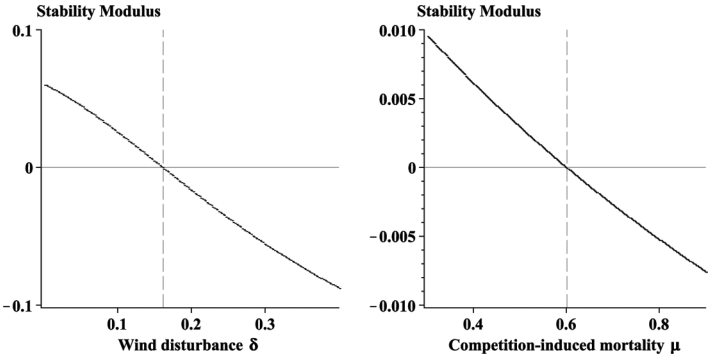

Figure 4. Stability modulus of the Jacobian matrix of System {(24),(25),(26),(27),(28)} linearized around the equilibria $(x^*, 0, 0, v^*, w^*)$ parameterized by δ (left panel) and μ (right panel). Parameters: $d_I = d_M = 0.01$, $\beta = g = 0.2$, $\mu = 0.1$ (left) and $\delta = 0.12$ (right). The dashed vertical line in each panel corresponds to the critical value $\delta_c \approx 0.16186$ (left) and $\mu_c \approx 0.60152$ (right).

3.3. Early Dynamics of Colonization

To have an interpretation of why the re-scaled extinction equilibrium has strictly positive components is useful to examine the early dynamics of some local densities at the beginning of the colonization of an empty area, when almost all the sites are gaps. As in Garcia-Domingo and Saldaña (2011), we derive the limit equations for the dynamics of the local densities as $[O]/N \to 1$ by assuming that x tends to an arbitrary but fixed value $\xi > 0$ as $[O]/N \to 1$ because $x^* > 0$ at any extinction equilibrium. Using $[OM]/(z[O]) \to 0$ as $[O]/N \to 1$, from Eq. (4) and (6),

$$\begin{aligned}\frac{d}{dt}\left(\frac{[II](t)}{z[I](t)}\right) &= \frac{[II]\prime(t)}{z[I](t)} - \frac{[II](t)}{z[I](t)}\frac{[I]\prime(t)}{[I](t)} \\ &\to -\left(g + d_I + \beta\frac{[OM](t)}{z[M](t)}\frac{[M](t)}{[I](t)} + \mu\frac{z-2}{z}\frac{[IM](t)}{z[I](t)}\right)\frac{[II](t)}{z[I](t)}.\end{aligned} \tag{29}$$

The strict positivity of the term in parentheses implies that the local density $u(t) = [II](t)/(z[I](t))$ tends to 0 exponentially fast as $t \to \infty$. This fact is consistent with $[II]^*/(z[I]^*) = 0$ at the bifurcation point given by the survival-extinction transition. As $x(t) > 0$ for all $t > 0$ and $[II](t)/(z[I](t))$ tends to 0 with time when $[O]/N \approx 1$, $u(t) = x(t)\,[II](t)/(z[I](t))$ also tends to 0 with time, and the limit equation of Eq. (27) is:

$$\begin{aligned}v\prime(t) &= \frac{\beta}{z}(1 - w(t)) \\ &\quad - \left(g(1+\xi) + d_I + \frac{\mu}{z} + \mu k\frac{v(t)}{\xi} + \frac{\beta}{z} - \frac{\delta}{z}(1 - v(t) - w(t))\right)v(t).\end{aligned} \tag{30}$$

From the phase portrait of the system given by Eq. (28) and (30) (with $x = \xi$), this limit system has always a unique equilibrium $(v_O^*, w_O^*) \in \{(v, w) \in (0,1) \times (0,1) : v + w < 1\}$, and $v(t)$ and $w(t)$ are always strictly positive. Even if we are very close to the extinction equilibrium, the densities $[IM]/(z[M])$ and $[MM]/(z[M])$ of immature and mature trees around a mature tree grow quickly. These local densities settle the environmental conditions that will determine the initial success or failure of the colonization of an empty area. Moreover, under a general condition on the parameters values (independent of ξ), the asymptotic stability of (v_O^*, w_O^*) is guaranteed (see Appendix).

When the extinction equilibrium is unstable, the assumption $[O]/N \to 1$ is no longer true as the colonization progresses. This means that our previous analysis based on the limit equations is no longer valid and the full system must be considered.

4. SIMULATIONS

To check the validity of the model predictions, we performed simulations with cellular automata (CA) using the transition rates described in section 2. The size of the lattice is 100×100; periodic conditions are assumed at the boundaries and the size of the neighborhood of each site is $z = 4$. The tuning parameters in the simulations are, alternatively, the competition-induced mortality rate μ of immature trees

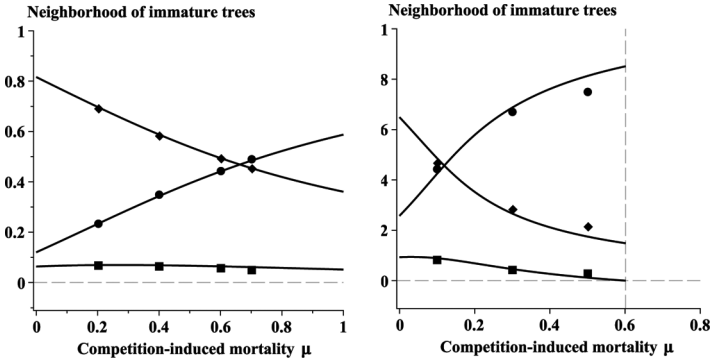

Figure 5. Local densities around immature trees at equilibrium parameterized by μ: $[OI]/(z[I])$ (increasing curve), $[IM]/(z[I])$ (decreasing curve) and $[II]/(z[I])$ (the lowest curve). Circles, squares, and diamonds result from the simulations of the CA model. Parameters: $\beta = 0.2$, $g = 0.2$, $d_I = d_M = 0.01$, $\delta = 0.05$ (left panel), and $\delta = 0.12$ (right panel). The dashed vertical line in the right panel corresponds to the critical value $\mu_c \approx 0.60152$.

and the additional mortality δ of the mature trees due to wind disturbance. The other parameters are kept constant at: $g = \beta = 0.2$ and $d_I = d_M = 0.01$. All values of δ and μ used in the CA satisfy the inequalities $g + d_I + \mu \leq 1$ and $d_M + \delta \leq 1$. These constraints and the additional one given by $\beta \leq 1$ imply that, at each time step of the simulations, the probability that a given transition takes place in a given lattice site x is equal to the corresponding transition rate defined in section 2. The initial configuration consists of approximately one third of the sites in each of the three possible states which are randomly distributed over the lattice.

The simulations show a good agreement among the local densities predicted by the pair approximation and those observed in the CA when parameters are far from the survival-extinction transition (Figures 5 and 6). The disagreement between predictions and simulations of CA for parameters close to the critical values is

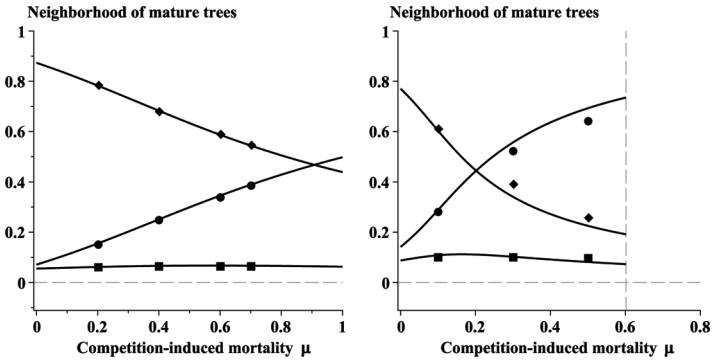

Figure 6. Local densities around mature trees at equilibrium parameterized by μ: $[OM]/(z[M])$ (increasing curve), $[IM]/(z[M])$ (decreasing curve) and $[MM]/(z[M])$ (the lowest curve). Circles, squares, and diamonds result from the simulations of the CA model. Parameters: $\beta = 0.2$, $g = 0.2$, $d_I = d_M = 0.01$, $\delta = 0.05$ (left panel), and $\delta = 0.12$ (right panel). The dashed vertical line in the right panel corresponds to the critical value $\mu_c \approx 0.60152$.

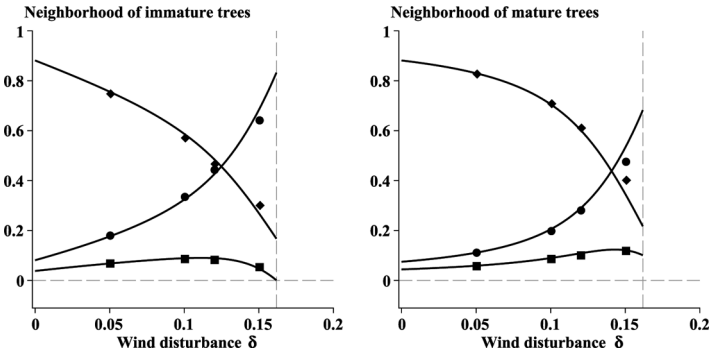

Figure 7. Local densities around immature (left) and mature (right) trees at equilibrium parameterized by δ. Left panel: $[OI]/(z[I])$ (increasing curve), $[IM]/(z[I])$ (decreasing curve) and $[II]/(z[I])$ (the lowest curve). Right panel: $[OM]/(z[M])$ (increasing curve), $[IM]/(z[M])$ (decreasing curve) and $[MM]/z[M]$ (the lowest curve). Circles, squares, and diamonds result from the simulations of the CA model. Parameters: $\beta = 0.2$, $g = 0.2$, $d_I = d_M = 0.01$, $\mu = 0.1$. The dashed vertical line in the panels corresponds to the critical value $\delta_c \approx 0.16186$.

known (Matsuda et al., 1992; Sato et al., 1994; Levin and Durrett, 1996; Tilman and Kareiva, 1997). It occurs because of long-range spatial correlations between the site states. When μ is used as a tuning parameter, predictions about local densities close to extinction are slightly less accurate than those obtained when δ is the tuning parameter (Figure 7).

The effect of the competition-induced mortality μ on the spatial arrangement of trees is only noticeable for $\delta > 0$. In this case, there is a lower bound for μ over which an empty site is more likely in the neighborhood of an immature tree than around a mature tree. Meanwhile, the probability of having another immature tree in the neighborhood tends to 0 smoothly. This effect of μ is greater for large values of δ (as the comparison between the left and right panels of Figure 5 shows).

5. CONCLUSION

Our pair-approximation model of the spatial distribution of a forest close to extinction shows that the competition-induced mortality μ of immature trees caused by mature trees is less determinant for an initial success of colonization in an empty area than wind disturbance δ.

Close to extinction, the agreement between model predictions and simulations from cellular automata is lower than in the case where mature trees affect the growth of immature trees by reducing sun-light availability but not survival (Garcia-Domingo and Saldaña, 2011). The stronger interaction among mature and immature trees assumed in the present model and the fact that δ must be large enough for having reasonable critical values of μ might be the reason.

The effect of competition-induced mortality μ is to reinforce the effect of wind disturbance δ when the system approaches the survival-extinction transition. In particular, because we assumed very low natural mortalities for mature and immature trees in the simulations ($d_I = d_M = 0.01$), this effect, to be noticeable for realistic values of μ_c, requires that $\delta \gg 0$ (top right panel in Figure 3). When $\mu \to \mu_c$, as well as

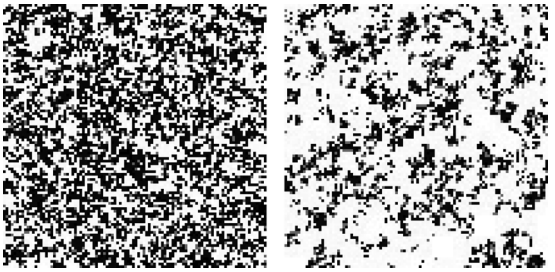

Figure 8. Final configurations after $T = 1000$ transitions of the CA model. Left panel: $\delta = 0.05$ and $\mu = 0.66$. For these values, the neighborhood of immature trees satisfies that $[OI]/(z[I]) \approx [IM]/(z[M])$ but the system is far from extinction. Right panel: $\delta = 0.15$ (close to the critical vale) and $\mu = 0.05$. In this panel the segregation between immature and mature trees is more obvious. The initial configuration is taken randomly satisfying that one third of the sites are in each of the three possible states. White, grey, and black sites correspond to gaps, immature trees, and mature trees, respectively. In both panels, $g = 0.2$, $\beta = 0.2$, and $d_I = d_M = 0.01$.

when $\delta \to \delta_c$, immature trees show a trend to be located between mature trees and gaps (Figure 8). In the first case, immature trees minimize the competition effects caused by mature trees while, in the second one, mature trees avoid the effect of wind disturbance. When $\mu \to \mu_c$, the neighborhoods of mature and immature trees change less abruptly (Figures 5 and 6) than when $\delta \to \delta_c$ (Figure 7).

ACKNOWLEDGMENTS

The authors thank two anonymous referees for their comments. This work was partially supported by the research projects MTM2008-06349-C03-02 (J.L.G-D, J.S.) and MTM2011-27739-C04-03 (J.S.) of the Spanish government and 2009SGR-345 of the Generalitat de Catalunya (J.S.).

REFERENCES

Adams, T.P., Purves, D.W., and Pacala, S.W. (2007). Understanding height-structured competition in forests: is there an R^* for light? *Proceedings of the Royal Society B*, *274*: 3039–3047.

Bascompte, J. and Solé, R.V. (Eds.), (1997). *Modelling Spatiotemporal Dynamics in Ecology*. New York: Springer.

Chen, Q., Mynett, A.E., and Minns, A.W. (2002). Application of cellular automata to modelling competitive growths of two underwater species Chara aspera and *Potamogeton pectinatus* in Lake Veluwe. *Ecological Modelling*, *147*: 253–265.

Childress, M. (1997). Predicting dynamics of spatial automata models using Hamiltonian equations. *Ecological Modelling*, *96*: 293–303.

Cronhjort, M.B. (2000). The interplay between reaction and diffusion. In U. Dieckmann, R. Law, and J.A.J. Metz (Eds.), *The Geometry of Ecological Interactions*. Cambridge: Cambridge University Press, pp. 151–170.

Dekker, M., Sass-Klaassen, U., and den Ouden, J. (2009). The effect of canopy position on growth and mortality in mixed sapling communities during self-thinning. *European Journal of Forest Research*, *128*: 455–466.

Ellner, S. (2001). Pair approximation for lattice models with multiple interaction scales. *Journal of Theoretical Biology*, *210*: 435–447.
Garcia-Domingo, J.L. and Saldaña, J. (2011). Extinction threshold for spatial forest dynamics with height structure. *Journal of Theoretical Biology*, *276*: 138–149.
Goetz, R.U., Xabadia, A., and Calvo, E. (2011). Optimal forest management in the presence of intraspecific competition. *Mathematical Population Studies*, *18*: 151–171.
Gratzer, G., Canham, C. and Dieckmann, U., et al. (2004). Spatio-temporal development of forests—current trends in field methods and models. *Oikos*, *107*: 3–15.
Guckenheimer, J. and Holmes, P. (1983). *Nonlinear Oscillations, Dynamical Systems, and Bifurcations of Vector Fields* 1st ed. New York: Springer-Verlag.
Hanski, I. (1999). *Metapopulation Ecology*. New York: Oxford University Press.
Harada, Y., Ezoe, H., and Iwasa, Y., et al. (1995). Population persistence and spatially limited social interaction. *Theoretical Population Biology*, *48*: 65–91.
Harada, Y. and Iwasa, Y. (1994). Lattice population dynamics for plants with dispersing seeds and vegetative propagation. *Research on Population Ecology*, *36*: 237–249.
Hiebeler, D. (2005). Spatially correlated disturbances in a locally dispersing population model. *Journal of Theoretical Biology*, *232*: 143–149.
Hubbell, S.P., Foster, R.B., and O'Brien, S.T., et al. (1999). Light-gap disturbances, recruitment limitation, and tree diversity in a neotropical forest. *Science*, *283*: 554–557.
Keeling, M. (1999). The effects of local spatial structure on epidemiological invasions. *Proceedings of the Royal Society London B*, *266*: 859–867.
Kubo, T., Iwasa, Y., and Furumoto, N. (1996). Forest spatial dynamics with gap expansion: Total gap area and gap size distribution. *Journal of Theoretical Biology*, *180*: 229–246.
Levin, S.A. and Durrett, R. (1996). From individuals to epidemics. *Philosophical Transactions of the Royal Society of London B*, *351*: 1615–1621.
Li, B-L., Wu, H., and Zou, G. (2000). Self-thinning rule: A causal interpretation from ecological field theory. *Ecological Modelling*, *132*: 167–173.
Manrubia, S.C. and Solé, R.V. (1997). On forest spatial dynamics with gap formation. *Journal of Theoretical Biology*, *187*: 159–164.
Martin, P.H., Canham, C.D., and Kobe, R.K. (2010). Divergence from the growth–survival trade-off and extreme high growth rates drive patterns of exotic tree invasions in closed-canopy forests. *Journal of Ecology*, *98*: 778–789.
Matsuda, H., Ogita, N., Sasaki, A., et al. (1992). Statistical mechanics of population—The lattice Lotka-Volterra model. *Progress in Theoretical Physics*, *88*: 1035–1049.
Metz, J.A.J. and Diekmann, O. (1986). *The Dynamics of Physiologically Structured Populations. Springer Lecture Notes in Biomathematics*. Heidelberg: Springer–Verlag.
Pagnutti, C., Anand, M., and Azzouz, M. (2005). Lattice geometry, gap formation and scale invariance in forests. *Journal of Theoretical Biology*, *236*: 79–87.
Pagnutti, C., Azzouz, M., and Anand, M. (2007). Propagation of local interactions create global structure and dynamics in a tropical rainforest. *Journal of Theoretical Biology*, *247*: 168–181.
Rand, D.A. (1999). Correlation equations and pair approximation for spatial ecologies. In J. McGlade (Ed.), *Advanced Ecological Theory*. Oxford: Blackwell Science, pp. 100–142.
Sato, K., Matsuda, H., and Sasaki, A. (1994). Pathogen invasion and host extinction in lattice structured populations. *Journal of Mathematical Biology*, *32*: 251–268.
Sato, K. and Iwasa, Y. (2000). Pair approximations for lattice-based ecologies In U. Dieckmann, R. Law and J.A.J. Metz (Eds.), *The Geometry of Ecological Interactions*. Cambridge: Cambridge University Press, pp. 341–358.
Schlicht, R. and Iwasa, Y. (2004). Forest gap dynamics and the Ising model. *Journal of Theoretical Biology*, *230*: 65–75.

Schlicht, R. and Iwasa, Y. (2007). Spatial pattern analysis in forest dynamics: Deviation from power law and direction of regeneration waves. *Ecological Research*, *22*: 197–203.
Silvertown, J., Holtier, S., Johnson, J., et al. (1992). Cellular automaton models of interspecific competition for space—the effect of pattern on process. *Journal of Ecology*, *80*: 527–534.
Solé, R.V., Bartumeus, F., and Gamarra, J.G.P. (2005). Gap percolation in rainforests. *Oikos*, *110*: 177–185.
Solé, R.V. and Manrubia, S. (1995). Are rainforests self-organized in a critical state? *Journal of Theoretical Biology*, *173*: 31–40.
Tahvonen, O. (2004). Optimal harvesting of forest age classes: A survey of some recent results. *Mathematical Population Studies*, *11*: 205–232.
Tilman, D. and Kareiva, P. (1997). *Spatial Ecology: The Role of Space in Population Dynamics and Interspecific Interactions*. Princeton: Princeton University Press.

APPENDIX

The phase portrait of the limit system is defined by Eq. (28) and (30) for a fixed ratio $x=\xi$ between immature and mature trees. We have seen that $x^*>0$ and $0<v^*+w^*<1$ at any equilibrium of Eq. (24), (25), (26), (27), and (28) of the form $(x^*, 0, 0, v^*, w^*)$. Assume that x approaches an arbitrary but fixed value $\xi>0$ when $[O]/N\to 1$. The nullclines $v'(t)=0$ and $w'(t)=0$ of the system are given by the curves:

$$w_1(v)=\frac{z}{\delta v+\beta}\left(\frac{\beta}{z}-v\left(g(1+\xi)+d_I+\frac{\mu}{z}+k\mu\frac{v}{\xi}+\frac{\beta}{z}-\frac{\delta}{z}(1-v)\right)\right), \tag{31}$$

$$v_2(w)=\frac{w\left(g\xi+d_M+\frac{z-2}{z}\delta(1-w)\right)}{2g+\frac{z-2}{z}\delta w}. \tag{32}$$

Then $w_1(v)$ is a strictly decreasing function for all $v\in[0, 1]$ with $w_1(0)=1$ and $w_1(1)<0$, which does not intersect the straight line $v+w=1$ for $v\in(0, 1)$ because $w_1''(v)<0$ and $w_1'(0)<-1$. Also, $v_2(w)$ is strictly positive for all $w\in(0, w_0)$ with $w_0=1+(g\xi+d_M)/(\delta(z-2)/z)>1$. Moreover, $v_2(0)=v_2(w_0)=0$ and

$$v_2''(w)=-4g\frac{z-2}{z}\delta\frac{2g+g\xi+d_M+\frac{z-2}{z}\delta}{\left(2g+\frac{z-2}{z}\delta w\right)^3}<0\quad\forall\, w>0. \tag{33}$$

For any $\xi>0$, there always exists a unique strictly positive equilibrium $(v_O^*, w_O^*)\in\Omega:=\{(0,1)\times(0,1): v+w<1\}$ of System {(28),(30)}.

The Jacobian matrix of this limit system is $J(v,w)=\begin{pmatrix} a_{11} & a_{12}\\ a_{12} & a_{22}\end{pmatrix}$ with

$$a_{11}=-\left(g(1+\xi)+d_I+\frac{\mu}{z}+\frac{\beta}{z}-\frac{\delta}{z}(1-v-w)\right)-v\left(2k\frac{\mu}{\xi}+\frac{\delta}{z}\right) \tag{34}$$

$$a_{12}=-\frac{\beta}{z}-\frac{\delta}{z}v, \tag{35}$$

$$a_{21}=2g+\frac{z-2}{z}\delta w, \tag{36}$$

$$a_{22} = -\left(g\xi + d_M + \frac{z-2}{z}\,\delta(1-v-w)\right) + \frac{z-2}{z}\delta w. \tag{37}$$

From $\xi > 0$ and $0 < v + w < 1$, for $z \geq 4$,

$$\begin{aligned}
\text{trace}(J) &< \frac{z-2}{z}\delta w - \left(g + d_I + d_M + \frac{\mu}{z} + \frac{\beta}{z} + \frac{z-3}{z}\delta(1-v-w) + \frac{\delta}{z}v\right) \\
&= ((2z-5)w + (z-4)v - (z-3))\frac{\delta}{z} - \left(g + d_I + d_M + \frac{\mu}{z} + \frac{\beta}{z}\right) \\
&< ((2z-5)w + (z-4)(1-w) - (z-3))\frac{\delta}{z} - \left(g + d_I + d_M + \frac{\mu}{z} + \frac{\beta}{z}\right) \\
&< (z-2)\frac{\delta}{z} - \left(g + d_I + d_M + \frac{\mu}{z} + \frac{\beta}{z}\right)
\end{aligned} \tag{38}$$

for all $(v, w) \in \Omega$. Hence, a sufficient condition for having trace $(J) < 0$ at any $(v, w) \in \Omega$ is:

$$(z-2)\frac{\delta}{z} < g + d_I + d_M + \frac{\mu}{z} + \frac{\beta}{z}, \tag{39}$$

which we interpret as an upper bound for the wind disturbance δ in terms of the other parameters and the spatial geometry of the lattice defined by z.

This condition guarantees the nonexistence of periodic orbits lying entirely in Ω by Bendixson's criterion (Guckenheimer and Holmes, 1983). When it is combined with the vector field of the system, the asymptotic stability of the equilibrium (v_O^*, w_O^*) follows. For $z = 4$ (the neighborhood size used in our simulations) and for $z = 8$ (the so-called Moore neighborhood), condition (39) is fulfilled even by values of δ larger than the critical value δ_c computed from the parameter values used in the simulations (see Figure 2 for $z = 4$).